Journal of the Korean Vacuum Society
Vol. 8, No. 4(2), December 1999, pp. 519~523

Epitaxial thickness during low-temperature Si(001) growth: effect of substrate vicinality

N.-E. Lee

Department of Materials Engineering, Sungkyunkwan University, Suwon 440-746, Korea

(Received December 18, 1999)

저온 Si(001) 저온 성장중 에피텍시 두께: 기판 vicinality의 영향

이내응

성균관대학교 재료공학과

(1999년 10월 18일 접수)

Abstract – Epitaxial thickness $t_e(T_s)$ of Si films grown at the substrate temperature $T_s = 80\sim300^{\circ}C$ by ultra-high vacuum ion-beam sputter deposition onto nominally-singular, [100]-, and [110]-miscut Si(001) was measured. $t_e(T_s)$ values of films grown on vicinal Si(001) substrates were decreased compared to those of films grown on nominally-singular Si(001). Evolution of surface roughness measured by atomic force microscopy of films grown at 300°C showed that the increased step density in vicinal substrates increases the tendency toward unstable growth resulting in larger surface roughness, which in turn decreases t_e.

요 약 – 초고진공 이온빔 스퍼터 장치를 이용하여 80~300°C의 기판온도(T_s) 범위에서 실리콘 기판의 정상 (001)면과 [100] 및 [110] 방향으로 기울어진 vicinal (001)면위에 성장된 실리콘 박막의 에피텍시 두께 $t_e(T_s)$를 측정하였다. vicinal 기판위에 성장된 실리콘 박막의 에피텍시 두께 $t_e(T_s)$가 정상 (001)면에 성장시킨 경우에 비교하여 감소하였다. 300°C의 기판온도에서 박막의 성장두께에 따른 표면조도의 변화를 atomic force microscopy을 이용하여 측정결과로 부터 vicinal 기판위의 증가된 step 밀도가 표면 조도를 증가시키어 불안정 성장 경향을 증대시키고 이것이 에피텍시 두께를 감소시키는 원인으로 작용하였음을 알 수 있었다.

1. Introduction

Thin film applications demand ever lower growth temperatures in order to, for example, obtain abrupt interfaces in multilayer devices, minimize alloy and dopant interlayer diffusion, and inhibit phase transitions in metastable materials. Epitaxy at very low temperature proceeds under conditions where a significant fraction of adatoms condensing on the tops of islands cannot cross step edges to lower terraces before being joined by another adatom and nucleating a new higher-level island. As growth continues in the low adatom mobility two-dimensional (2D) multilayer mode, the roughness of growth front gradually increases.

Since continued growth at very low growth temperature leads to an increasingly rough surface with a non-reversible transition to amorphous-layer deposition [1-4], the roughening rate of growth front clearly plays a decisive role in determining the extent of epitaxy during multilayer growth. Increased surface roughening rate caused by the presence of impurities such as H [1,5] and Sb [6], for example, has been shown to decrease t_e for MBE and ion-beam sputter deposited low-temperature Si, respectively. Therefore, smoothening of growth fronts is expected to increase epitaxial thickness t_e.

An initiative of the experiments presented in this experiment was to increase t_e by reducing the roughening rate by the use of vicinal substrates with smaller average terrace width λ because reduced λ is expected to facilitate the smooth film growth in the layer-by-layer or in the step-flow growth regime [7]. Contrary to the expectation, however, t_e of Si layers on [100]- and [110]-miscut Si(001) substrates was decreased compared to that of Si layers on nominally-singular Si(001) substrate. The surface roughness evolution of Si(001) layers grown on substrates with different miscut angles at 300°C by atomic force microscopy (AFM) measurements showed increased surface roughening rate in the layers grown on miscut Si(001) substrates than on nominally-singular Si(001) substrate and, in turn, decreased epitaxial thickness, t_e.

2. Experiment

All film growth experiments were conducted in a three-chamber load-locked 1×10^{-10} Torr UHV system with facilities for reflection high energy electron diffraction (RHEED), residual gas analysis, and Auger electron spectroscopy (AES). Sputtering was carried out using an UHV double-grid multi-aperture broad ion-beam source with the extracted beam focused by a postextraction unipotential electrostatic ion lens. High-purity energetic Si beams, with average Si atom energies of ~18 eV, were generated by bombarding an undoped 10-cm-diameter float-zone Si(001) wafer using a 1 keV ultra-high purity Kr^+ ion beam [4]. Incorporated metallic impurity concentrations were below secondary ion mass spectrometry detection limits ($\sim1\times10^{15}$-10^{16} cm^{-3}).

The primary substrates used in these experiments were Si(001) 2×1 wafers either nominally-singular, with miscuts as measured by high-resolution x-ray diffraction of 0.16° toward [110] corresponding to an average terrace width of 50 nm, or vicinal with miscuts of 4° toward [110] ($\lambda = 2$ nm) and 4° toward [100] ($\lambda = 2$ nm). The Si(001)-4° [100] surface consists of terraces bounded by single-atom height steps composed of equal fractions of A- and B-type edges. Substrate preparation consisted of degreasing followed by a UV ozone treatment, H passivation in dilute HF, degassing in UHV at 200°C for 1 h, oxide desorption at 700°C for 10 sec, and the growth of 100-nm-thick Si buffer layers. Buffer layer growth temperatures were chosen to be 650°C on singular and Si(001)-4° [110] substrates and 600°C on Si(001)-4° [100] substrate in order to obtain comparably smooth starting surfaces with nearly equal short-range roughnesses as judged by AFM measurements. No residual C or O was detected by AES. AFM measurements were carried out in air using a Digital Instruments Nanoscope II with oxide-sharpened Si_3N_4 tips whose radii were 5-40 nm. Transmission electron microscopy (TEM) and cross-sectional TEM (XTEM) analyses were performed using Philips CM-12 and Hitachi 9000 microscopes operated at 120 and 300 kV, respectively.

3. Results and Discussion

A series of Si layers with different film thicknesses was grown at $T_s = 80$~300°C with $R = 0.1$ nm-s^{-1} on the substrates with different miscut angles. XTEM micrographs of the films grown on vicinal substrates exhibit the same general features as those from the samples grown on nominally-singular Si(001) substrate over the entire temperature range as previously shown elsewhere [4]. The transition region between the defective epitaxial region and the amorphous phase is rough, consisting of truncated rectangular islands with facets, primarily {111}. Average total epitaxial thicknesses t_e which are the mean value of film thicknesses measured from the substrate/film interface to the midpoint of the

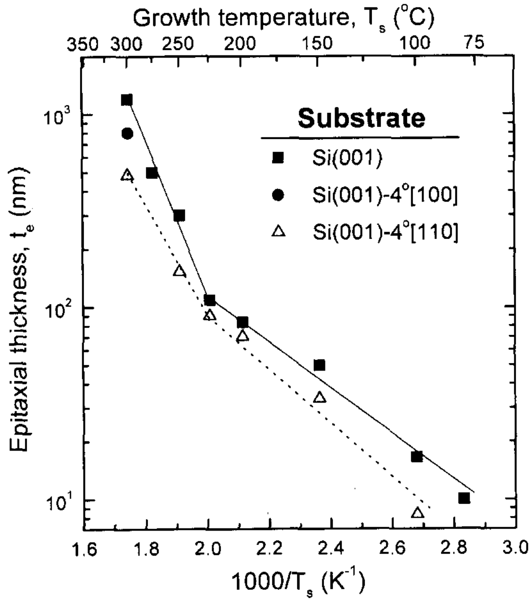

Fig. 1. Epitaxial thickness t_e of Si(001) films, grown on the substrates with different miscut angles using $\langle E\rangle_{Si}$ ~18 eV Si beams, as a function of T_s with $R = 0.1$ nm-s^{-1}.

crystalline-amorphous transition region were determined from XTEM or high-resolution XTEM micrographs, using observations from more than 20 different regions of each sample. Data for $t_e(T_s)$ are plotted for films grown on different substrates in Fig. 1. A decrease in the slope of $\ln(t_e)$ vs $-1/T_s$ at $T_s < 225^{\circ}C$ was explained in terms of changes in average island sizes giving rise to corresponding changes in interlayer mass transport [4]. t_e values of films on vicinal substrates were decreased, for example, to ~500 nm on Si(001)-4° [110] and ~800 nm on Si(001)-4° [100] from ~1200 nm on nominally-singular substrate at $T_s = 300^{\circ}C$. Decrease in t_e of films on Si(001)-4° [110] compared to t_e of those on singular substrate was observed for the entire growth temperature range investigated. These results are quite surprising because reduced terrace width of vicinal substrates is expected to facilitate smooth film growth due to reduced growth temperature required for step-flow growth [7].

To elucidate the effect of higher step density in vicinal substrates on surface roughening affecting t_e over the temperature range investigated in these experiments, surface roughness evolution with film thickness t was investigated for films grown on different substrates at $T_s = 300^{\circ}C$. AFM images (not shown here) of the Si(001) surfaces of films grown on singular and vicinal Si(001) substrates showed the gradual development of features, from linearly anisotropic along [110] to compact mound or pyramid-like structures [6,8,13] with film thickness t increasing. The initiation of feature development is faster on the [100]- and [110]-miscut vicinal substrates. The behavior on the [110]-miscut surface is similar to that on the [100]-miscut surface except that the mounds exhibit a strong shape anisotropy along the initial [110] step direction.

To obtain the root-mean squared (rms) surface roughness w, the height difference correlation function $G(\rho, t) = \langle |h(j, t) - h(i, t)| \rangle^2$ where ρ is the separation of positions i and j, was first calculated from raw AFM data. Saturated root-mean squared correlated height-difference $[G(\rho \rightarrow \infty, t)]^{1/2}$ is related to rms surface roughness w, $[G(\rho \rightarrow \infty, t)]^{1/2} \sim (w)^{1/2}$, where $w = [h^2 - \langle h \rangle^2]^{1/2}$ [9]. $[G(\rho \rightarrow \infty, t)]^{1/2}$ is defined here as the average of all measured G values obtained for ρ larger than that corresponding to the intersection of best-fit straight lines drawn through the steeply rising and saturation regions of $[G(\rho, t)]^{1/2}$ vs ρ data as seen in Fig. 2. As an example, $[G(\rho, t)]^{1/2}$ vs ρ plot for [110]-miscut surfaces are presented in Fig. 2.

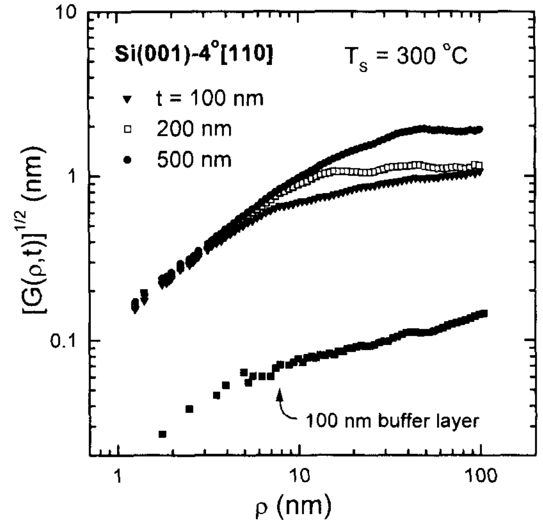

Fig. 2. Root-mean correlated height-difference $[G(\rho, t)]^{1/2}$ vs the separation ρ of positions i and j on the surfaces of Si films grown at 300°C with thicknesses t on Si(001)-4°[110] substrates.

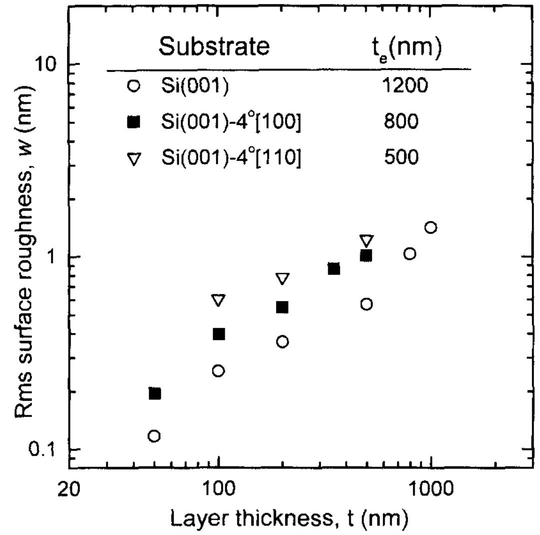

Fig. 3. Root-mean squared surface roughness w vs film thickness t for Si films grown at $T_s = 300^{\circ}C$ on nominally-singular Si(001), Si(001)-4° [100], and Si(001)-4° [110] substrates.

Calculated rms surface roughness w is plotted as a function of film thickness t in Fig. 3 together with epitaxial thickness t_e values at $T_s = 300°C$. Temporal evolution of surface roughnesses roughly follows a power-law dependence, $w \sim t^{\beta}$, rather than a linear dependence, where β is close to ~0.6-0.7. Other measurements of surface roughness evolution during Si(001) low-temperature epitaxy using MBE showed a power-law dependence from the roughness measurements by XTEM [10] and RHEED [11] or a linear dependence by RHEED [12]. The discrepancies between different experimental measurements including these results are not clearly understood at this point because of the use of different growth techniques, measurement methods, film thickness and growth temperature range investigated. An additional observation is that rms surface roughness w of films grown on vicinal substrates is larger compared to those on singular substrate at a given comparable film thickness t as seen in Fig. 3. In addition, epitaxial thickness t_e is disproportionately decreased with rms surface roughness w increasing as indicated in the Fig. 3. From these results, decreased t_e values of films on vicinal substrates are primarily attributed to increased surface roughening rate of films grown on vicinal substrates by the earlier development of mound structures caused by instability of growing film surface.

The use of vicinal substrates in these experiments, in which the average terrace width λ is of the order of adatom mean free paths (estimated, based upon data in reference 14, to be 2-3 nm at 300°C), would be expected to lead toward stable step-flow growth mode rather than to the growth instabilities leading to surface roughening. However, mechanisms determining the growth instability condition are complicated due to the presence of a diffusion bias during growth caused by the asymmetry in interlayer transport across step edges [15,16]. For example, preferred incorporation of adatoms at the ascending steps rather than at the descending steps in the step-flow mode is predicted to stabilize a vicinal surface due to a uphill diffusion current while destabilize a singular surface by the onset of terrace nucleation leading to the production of mound or pyramid-like structures [15,16]. Instabilities leading to the roughening of surface have also been reported during low-temperature MBE of Ge [13] and Cu [17] in the 2D multilayer growth mode on near-singular (001) substrates. However, the role of steps in influencing the evolution of surface roughening in this 2D multilayer growth mode, where high terrace nucleation rates are expected, has not been addressed.

The primary source of the growth instability during low-temperature Si deposition on singular and miscut Si(001) surfaces is believed to stem from the anisotropy in diffusion along and across dimer rows [14] combined with adatom trapping [18] or a strong reflection barrier [19] near descending A-step edges leading to enhanced *extrinsic* island nucleation. In the case of the miscut substrates, where the step density is high, we expect that extrinsic island nucleation rates will far exceed the rate of *intrinsic* random terrace nucleation resulting in a larger roughness and in turn a smaller epitaxial thickness t_e. This tendency is consistent with these experimental results that, surprisingly, and contrary to the high temperature step-flow case, the use of vicinal substrates with higher step densities during low temperature epitaxy of Si(001) enhances growth instabilities leading to larger surface roughness w and, in turn, reduced epitaxial thickness t_e.

4. Conclusion

Epitaxial thickness $t_e(T_s)$ of Si films grown at the substrate temperature $T_s = 80\text{~}300°C$ by UHV ion-beam sputter deposition onto Si(001) with different miscuts was measured. $t_e(T_s)$ values of films grown on miscut Si(001) substrates were decreased compared to those of films grown on nominally-singular Si(001). The results suggest that decrease in t_e is correlated to the increased surface roughening rate of Si films on vicinal substrates caused by the increased tendency toward unstable growth in the presence of larger substrate vicinality.

Acknowledgement

The author thanks Professor J. E. Greene for his helpful discussions during this work.

References

[1] D. J. Eaglesham, J. Appl. Phys. **77**, 3579 (1995).

[2] D. J. Eaglesham, H.-J. Gossmann, and M. Cerullo, Phys. Rev. Lett. **65**, 1227 (1990).

[3] G. Xue, H. Z. Xiao, M.-A. Hasan, J. E. Greene, and H. K. Birnbaum, J. Appl. Phys. **74**, 2512 (1993).

[4] N.-E. Lee, G. A. Tomasch, and J. E. Greene, Appl. Phys. Lett. **65**, 3236 (1994).

[5] D. J. Eaglesham, F. C. Unterwald, H. Luftman, D. P. Adams, and S. M. Yalisove, J. Appl. Phys. **74**, 6615 (1993).

[6] N.-E. Lee and J. E. Greene, Appl. Phys. Lett. **67**, 2459 (1995).

[7] J. Y. Tsao, *Materials Fundamentals of Molecular Beam Epitaxy* (Academic Press, Boston, 1993) p. 239.

[8] N.-E. Lee, David G. Cahill, and J. E. Greene, Phys. Rev. B **53**, 7876 (1996).

[9] H.-N. Yang, G.-C. Wang, and T.-M. Lu, *Diffraction From Rough Surfaces and Dynamic Growth Fronts* (World Scietific, Singapore, 1993) p. 62.

[10] D. P. Adams, S. M. Yalisove, and D. J. Eaglesham, Appl. Phys. Lett. **63**, 3571 (1993).

[11] B. Gallas, I. Berbezier, J. Derrien, J. Ruiz, and V. A. Zagrebnov, J. Vac. Sci. Technol. B **16**, 1564 (1998).

[12] O. P. Karpenko, S. M. Yalisove, and D. J. Eaglesham, J. Appl. Phys. **82**, 1157 (1997).

[13] J. E. Van Nostrand, S. J. Chey, M.-A. Hasan, D. G. Cahill, and J. E. Greene, Phys. Rev. Lett. **74**, 1127 (1995).

[14] Y.-W. Mo and M. G. Lagally: Surf. Sci. **248**, 313 (1991); Y.-W. Mo, J. Kleiner, M. B. Webb, and M. G. Lagally, Surf. Sci. **268**, 275 (1992).

[15] J. Krug, M. Plischke, and M. Siegert, Phys. Rev. Lett. **70**, 3271 (1993).

[16] M. D. Johnson, C. Orme, A. W. Hunt, D. Graff, J. Sudijino, L. M. Sander, and B. G. Orr, Phys. Rev. Lett. **72**, 116 (1994).

[17] H.-J. Ernst, F. Fabre, R. Folkerts, and J. Lapujoulade, Phys. Rev. Lett. **72**, 112 (1994).

[18] Z. Zhang, Y.-T. Lu, and H. Metiu, Phys. Rev. B **46**, 1917 (1992).

[19] D. Srivastava and B. J. Garrison, Phys. Rev. B **47**, 4464 (1993).